JCTC Journal of Chemical Theory and Computation

Article

pubs.acs.org/JCTC

Density-Functional Errors in Alkanes: A Real-Space Perspective

Erin R. Johnson*

Chemistry and Chemical Biology, University of California, Merced, 5200 North Lake Road, Merced, California 95343, United States

Julia Contreras-García

Laboratoire de Chimie Théorique, 4 place Jussieu, F-75005, Paris, France

Weitao Yang

Department of Chemistry, Duke University, Durham, North Carolina 27708, United States and Department of Physics, Faculty of Science, King Abdulaziz University, P.O. Box 80203, Jeddah 21589, Saudi Arabia

ABSTRACT: Density-functional theory (DFT) approximations are known to give systematic errors for isodesmic reaction energies of *n*-alkanes to form ethane. Several explanations have been proposed, involving both the exchange or correlation nature of the problem and its distance range (i.e., medium-range or long-range interactions). In this work, a new isodesmic reaction is defined to demonstrate that the reaction energy differences originate from localized interactions between contiguous CH_2 units in the *n*-alkane, i.e., from 1,3 interactions. Furthermore, we introduce a real-space interpretation of the error based on changes in electron density, described by our recently developed Non-Covalent Interactions (NCI) method. The reduced density gradient has smaller values for noncovalent 1,3 interactions in *n*-alkane reactants compared to ethane products. The gradient contribution to the exchange energy is consequently reduced, giving a constant energy bias against each propane unit in an *n*-alkane. Differences in exchange energy for grid points within the NCI regions are shown to be responsible for the reaction-energy errors. This is also demonstrated to be the source of error in Diels–Alder addition barrier heights obtained with GGA-based hybrid functionals.

Quantum-mechanical electronic structure calculations provide fundamental information describing molecular structure, interactions, and potential energy surfaces necessary for molecular dynamics. While both conventional *ab initio* wave function methods and Kohn–Sham Density-Functional Theory (DFT) are highly successful approaches, DFT is the better candidate for large systems, such as nanomaterials and biomolecules, because of its greater computational efficiency.

However, it has been observed that DFT errors can grow with molecular size, even for simple reactions. A particularly striking example is the isodesmic reaction where *n*-alkanes are fragmented into ethane molecules:[1−5]

$$CH_3(CH_2)_nCH_3 + nCH_4 \rightarrow (n+1)C_2H_6 \quad (1)$$

While generalized-gradient approximation (GGA) functionals perform much better than the simpler local-density approximation (LDA) for the prediction of bond energies, isodesmic reactions conserve the number and type of bonds between reactants and products. We therefore expect substantial error cancellation and an accurate description of this isodesmic reaction with basically any type of functional, but this is far from being the case. While the LDA performs extremely well for this class of reaction, GGAs fail dramatically, giving reaction-energy errors of up to ca. 12 kcal/mol for *n*-octane. Selected DFT results[6−9] for this isodesmic reaction are shown in Figure 1, and comparable results have been reported in the literature for a wide range of functionals.[1−5] Similar problems have been observed for the isomerization of alkanes and other organic molecules.[10−14]

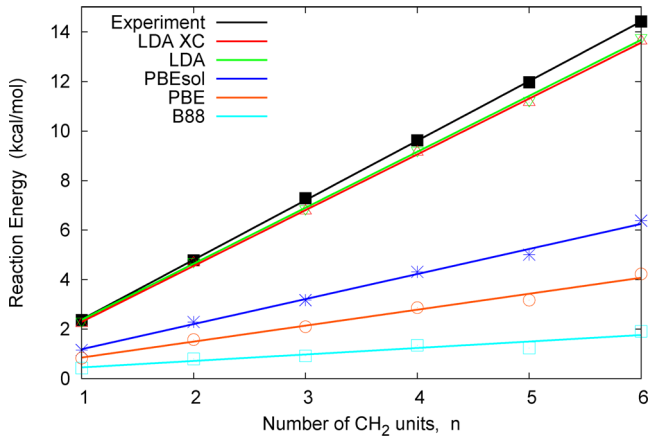

Figure 1. Isodesmic reaction energies (eq 1) for the *n*-alkane series from propane through octane. Values are expressed as a function of carbon chain length for the LDA exchange-correlation (XC) functional and exchange-only GGA functionals. Calculations were performed with the NUMOL program.[20] Experimental data were taken from ref 21.

Received: May 21, 2012
Published: July 17, 2012

Table 1. Errors in Calculated Isodesmic Reaction Energies (eq 1, 6, or 7) for *n*-Alkanes up to and including *n*-Octane[a]

method	eq 1	eq 6	eq 7
LDA XC	0.15	0.02	0.19
LDA	0.15	0.11	0.08
PBEsol	1.39	0.20	1.25
PBE	1.76	0.23	1.58
B88	2.14	0.20	1.98

[a]Results are shown for selected exchange-correlation (XC) or exchange-only functionals and are expressed as errors per propane unit (kcal/mol), relative to experimental results.[21]

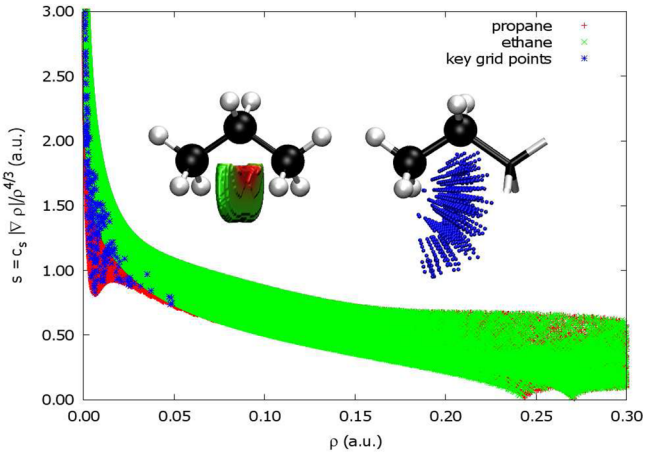

Figure 2. Reduced density gradient vs density plots for ethane and propane. Key grid points centered on the left-most CH_3 group, where the reduced gradient changes by 10% or more between ethane and propane, are highlighted. These points are plotted in real space for the propane molecule in the right inset. The left inset shows the noncovalent interaction region, which is an s = 1.5 au isosurface containing those points that fall below the lower edge of the propane $s(\rho)$ curve. Electron densities were calculated with B3LYP/6-31G*,[24−26] and isosurfaces were obtained using the NCIplot program.[17]

Table 2. Calculated Diels−Alder Barrier Heights (kcal/mol) for Selected Exchange-Correlation (XC) Functionals, Involving 25% Exact Exchange and PBE Correlation, Obtained from the NUMOL Program[a]

reaction	B88	PBE	PBEsol	CCSD(T)
ethylene + 1,3-cyclohexadiene	24.7	21.9	16.6	18.3
acetylene + 1,3-cyclohexadiene	24.9	22.3	17.2	19.0
ethylene + cyclopentadiene	20.0	17.3	11.8	13.5
acetylene + cyclopentadiene	21.8	19.4	14.3	16.2
mean absolute error	6.1	3.5	1.8	

[a]CCSD(T)/aug-cc-pVDZ barriers calculated using the Gaussian program[26] are shown for comparison.

This surprising result has given rise to much discussion within the DFT community. More complex functional forms, involving range-separation and dispersion[3,5,14] or excited-state information using MP2-based correlation energy terms (double-hybrid functionals),[4,10,11,13] can recover good agreement with experimental results for these isodesmic reaction energies. However, this does not solve the essential issue. That is, a clear identification of the source of the GGA errors is still needed to guide the development of improved functionals that maintain the computational speed of semilocal approximations.

Several explanations have been proposed, involving both the nature of the problem (exchange or correlation) and its distance range (medium-range or large-range interactions). Grimme has attributed this error to a neglect of medium-range correlation, related to a 1,3-protobranching interaction between methyl groups.[4] This interaction was thought to be a stabilizing interaction, rather than a steric interaction, which explains the greater stability of branched alkanes relative to linear alkanes.[10] The source of the error has alternatively been identified to lie in the exchange functional[15] involving a longer interaction range. The well-known failure of conventional DFTs to treat long-range van der Waals interactions is also important for this class of reaction. Dispersion corrections have been introduced by several authors;[3,4] however, it is commonly accepted that there is a deeper inherent problem with GGAs for these isodesmic reactions beyond dispersion.

In this contribution, we first introduce a new isodesmic reaction that will allow us to identify the interaction range. To investigate this problem from a real-space perspective, we turn to our Non-Covalent Interactions index (NCI),[16−18] based on the electron density and reduced gradient. Because this approach is directly linked to the difference between LDA and GGA exchange functionals, it enables insight into the chemical interpretation of DFT errors. Resorting to common densities in all cases, we will analyze the behavior of GGA exchange functionals for the NCI regions.

To understand the local source of the isodesmic error, we constrain our analysis to the LDA and GGA exchange functionals. The LDA exchange energy[6] is given by

$$E_X^{LDA} = -\frac{3}{2}\left(\frac{3}{4\pi}\right)^{1/3} \sum_\sigma \int \rho_\sigma^{4/3}\, d\mathbf{r} \tag{2}$$

This term is the first of the GGA gradient expansion:

$$E_X^{GGA} = E_X^{LDA} - \sum_\sigma \int F(s_\sigma)\, \rho_\sigma^{4/3}(\mathbf{r})\, d\mathbf{r} \tag{3}$$

The function $s = (1/C_F)|\nabla\rho|/\rho^{4/3}$, where $C_F = 2(3\pi^2)^{1/3}$, is known as the reduced density gradient and will be fundamental to our analysis. The function $F(s_\sigma)$ is most frequently expressed as one of two forms, the first of which is Becke's B88 functional:[9]

$$E_X^{B88} = E_X^{LDA} - \beta \sum_\sigma \int \rho_\sigma^{4/3} \frac{s_\sigma^2}{1 + 6\beta s_\sigma \operatorname{arcsinh}(s_\sigma)}\, d\mathbf{r} \tag{4}$$

where β is a constant. The second group of functionals uses the same functional form as in the PBE functional:[7]

$$E_X^{PBE} = E_X^{LDA} - \beta \sum_\sigma \int \rho_\sigma^{4/3} \frac{s_\sigma^2}{1 + \gamma s_\sigma^2}\, d\mathbf{r} \tag{5}$$

where β and γ are (different) constants. In this group, we can find Becke's 1986 functional[19] and the PBEsol method.[8] The PBEsol functional was designed to reproduce the exact second order gradient expansion of the exchange energy for a wider range of s values. As a consequence, the β parameter is smaller in PBEsol than in the original PBE formulation, which results in better performance for solid-state chemistry. It should also be noted that our notation for the PBE functional differs from the current literature[7] to allow direct comparison between the B88 and PBE functional forms. In the usual notation, the

dx.doi.org/10.1021/ct300412g | J. Chem. Theory Comput. 2012, 8, 2676−2681

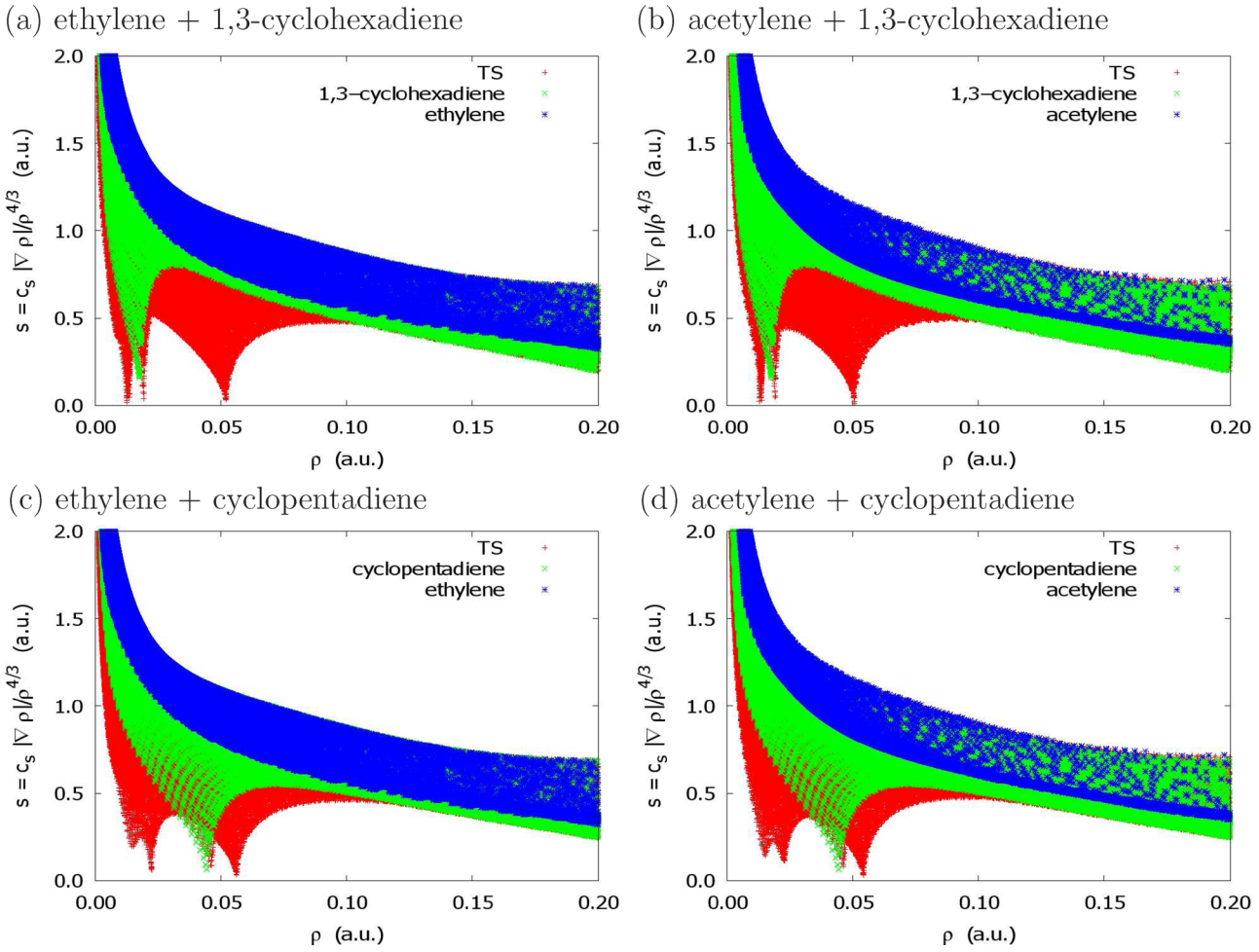

Figure 3. Reduced-gradient versus density plots for the transition states and separated reactants for each of the four selected Diels–Alder addition reactions.

enhancement factor in the PBE functional is written in terms of the parameters μ and κ as $F(s) = 1 + \kappa - \kappa/(1 + \mu s^2/\kappa)$.

In all of these cases, the gradient term lowers the GGA energy, relative to the LDA, and the degree of energy lowering increases with reduced gradient. The fact that LDA accurately describes the isodesmic reactions, whereas all GGAs fail to do so, implies incorrect behavior of the gradient expansion term. This observation is supported by the fact that isodesmic reaction-energy errors are reduced when PBEsol is used instead of PBE.[12]

To investigate the origin of the errors, we will consider four local DFT approximations: the LDA,[6] PBE,[7] PBEsol,[8] and B88[9] functionals. All calculations in this work were performed with the NUMOL program,[20] using self-consistent LDA densities.[6] The use of common densities enables all our DFT calculations to be compared on an equal footing and aids analysis of the relative exchange and correlation influences on the GGA error. Molecular geometries were obtained from the G3X reference set.[21]

From Figure 1, the LDA gives results in excellent agreement with experimental data.[21] Interestingly, the degree of error cancellation is sufficient that the exchange-only LDA gives reaction energies in very good agreement with reference data, and including the LDA correlation term has a negligible effect. However, GGAs miss the systematic error compensation seen with the LDA. These results suggest that the gradient contribution to the exchange term is responsible for the incorrect description of protobranching in isodesmic reactions, and the failure of GGAs is not a correlation effect. Thus, we can neglect the dynamical correlation functional and focus on differences in the exchange functionals.[15] Going from LDA to GGA exchange gives rise to large systematic errors, with the reaction energies consistently underestimated and the error increasing linearly with increasing chain length. The gradient term of these GGA functionals must either overstabilize the ethane fragments or destabilize methane and the long-chain *n*-alkanes. This is in agreement with the results of Grimme et al, who linked behavior of the gradient term with this failure of GGAs.[12]

To isolate the range of the interaction-energy errors, we consider the fragmentation of *n*-alkanes into both ethane (eq 1) and propane units according to the new isodesmic reaction

$$CH_3(CH_2)_nCH_3 + (n-1)C_2H_6 \rightarrow nC_3H_8 \qquad (6)$$

Whereas the isodesmic reaction in eq 1 highlights 1,3 interactions, comparison with results from eq 6 enables us to determine if even longer-range interactions are at play. Experimental data[21] give a reaction energy of 0.04 kcal/mol for butane in eq 6, increasing to 0.23 kcal/mol for *n*-octane. Therefore, this reaction is essentially thermoneutral, and besides a small contibution from dispersion, there are no significant long-range interactions stabilizing the *n*-alkane.

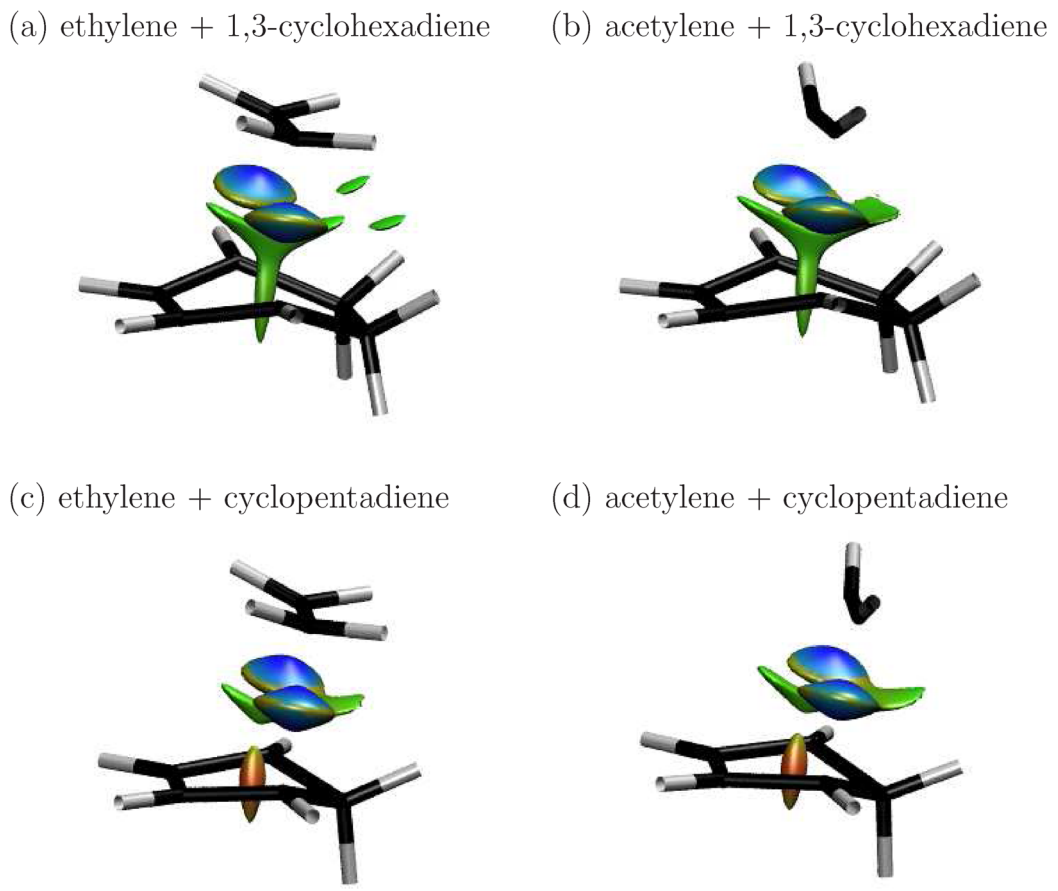

Figure 4. NCI isosurfaces (s = 0.45 au, with blue-green-red color scale for $-0.07 < \text{sign}\,(\lambda_2)\rho < 0.07$ au) for the transition states of each of the four selected Diels–Alder addition reactions.

For both isodesmic reaction schemes, the error in reaction energy per propane unit can be determined from the difference in slope, relative to experimental results. These values are collected in Table 1 for selected functionals. For eq 6, both GGAs and LDA are in good agreement with experimental data, showing that the error is localized to the 1,3 interaction between carbon atoms in propane and longer-chain alkanes. This has been termed the "protobranching" interaction in the literature.[2]

The importance of 1,3 interactions is made clear by adding the isodesmic reactions in eqs 1 and 6. This gives

$$n(CH_4 + C_3H_8 \rightarrow 2C_2H_6) \quad (7)$$

Therefore, the difference between eq 6 (where all functionals considered perform well) and eq 1 (where the GGAs fail to give chemical accuracy) is directly due to a systematic understabilization of the 1,3 interaction in propane. This explains almost exactly linear-scaling of the isodesmic reaction errors with the number of CH_2 units. Indeed, it can be seen from Table 1 that the errors in isodesmic reaction energies from eq 1 expressed per propane unit match the error for the $CH_4 + C_3H_8 \rightarrow 2C_2H_6$ reaction (eq 7) fairly closely, and the slightly larger errors for eq 1 are likely due to the neglect of dispersion,[22] which will contribute to the stability of the long-chain alkanes.

Since the DFT energy is determined from the ground-state electron density, it should, in principle, be possible to associate changes in energetics with changes in molecular density. We now consider an interpretation in which the systematic errors are traced back to real space. The regions of interaction are identified as those where the reduced electron-density gradient undergoes large changes between reactants and products.

Considering that, in GGAs, the exchange energy is determined from ρ and s, differences in energy between LDA and GGAs should originate principally from regions with large change in density or gradient between ethane and a larger n-alkane. These same two quantities form the basis for our recently-developed Non-Covalent Interactions (NCI) index, which allows characterization and visualization of both inter- and intramolecular interactions.[16,17] Because atomic densities are piecewise exponential, plots of s versus ρ have a characteristic shape corresponding to the form of $\rho^{-1/3}$. Covalent bonds appear at high density and low gradient (zero at the bond critical points). On the other hand, noncovalent interactions appear as troughs at low density and low gradient.

Plots of s versus ρ are shown in Figure 2 for ethane and propane, the smallest alkane that exhibits protobranching interactions. The distribution of density and gradient values is mostly the same for these two molecules. The only significant difference is an NCI region in propane, which appears as an additional shoulder at low density and low gradient. Plotting a reduced-gradient isosurface encompassing those points that lie below the lower edge of the ethane density-gradient curve gives the NCI surface shown in the inset of Figure 2. It is color-coded according to the density values at the isosurface and represents noncovalent interactions between the CH_3 groups in propane. This "protobranching" interaction between the 1,3-carbons in propane has been argued to be both stabilizing[2] and

destabilizing.[23] Our NCI calculations show that this interaction is characterized by points with a positive second Hessian eigenvalue, which indicates this to be a nonbonding interaction.[16,17]

For the reaction of propane and methane to form two ethane molecules (eq 7), roughly two-thirds of the reaction-energy difference between LDA and GGA functionals comes from integration points centered on the CH_3 groups (i.e., two out of three carbon units, since the CH_2 contribution is lacking). We performed a simple computational experiment to examine the real-space origin of the error. Calculations were performed on propane and on an ethane molecule fixed to overlay the CH_3CH_2 moiety. Considering the CH_3 group that is conserved, the DFT integration grid points for these atoms will have identical placements for both species. This allows direct comparison of the density, gradient, and exchange energy contribution at each grid point.

For this system, we identified the particular grid points where the reduced gradient decreases substantially between ethane and propane. There are only 1711 grid points where the reduced gradient decreases by more than 5% from ethane to propane and the contribution to the exchange energy is greater than 1×10^{-9} au. This represents only 2.2% of the 77 600 total grid points for the CH_3 group (100 radial points and 194 angular points per atom). This list can be truncated further by considering only the 906 points where the reduced gradient decreases by more than 10% from ethane to propane and the contribution to the exchange energy is greater than 1×10^{-7} au.

Once grid points with a large reduction in reduced gradient were identified, they were found to recover the vast majority of the difference between LDA and GGA reaction energies. Averaging over the three GGAs considered, 82.7% of the overall energy difference for the CH_3 groups was recovered counting only the 1711 points with $\Delta s > 5\%$. If only the 906 grid points with $\Delta s > 10\%$ are considered, 74.6% of the total energy difference is still recovered. Thus, only 1−2% of the total integration grid points are responsible for ca. 75−80% of the reaction-energy error. If these grid points are plotted in real space, as in Figure 2, they lie between the two CH_3 groups of propane, such that their locations match the NCI region. This demonstrates not only the locality of the interaction but also that the change in reduced gradient during formation of 1,3 interactions is indeed responsible for the poor behavior of GGA functionals for these isodesmic reactions.

These results imply that the origin of the GGA error for isodesmic reactions is the disappearance of low-density, low-gradient regions when proceeding from *n*-alkane reactants to ethane products. The contributions of these points to the isodesmic reaction energy can be understood by considering the exchange-energy expressions. While the density values are similar, the reduced gradient values are larger for ethane than propane, so the exchange energy will be lower. Therefore, propane is destabilized, relative to ethane, giving a systematic energy error for each propane unit in an *n*-alkane. By overstabilizing regions with high *s*, relative to low *s*, GGAs effectively overestimate the effect of repulsion between the 1,3-carbons in *n*-alkanes.

The reduced magnitude of the gradient term in PBEsol exchange is a first step in the correction of isodesmic errors though GGAs, but errors are still too large (see Figure 1). The inclusion of dispersion, long-range exact exchange, or MP2 correlation, each act to reduce this bias, restoring the good agreement with reference data obtained with the LDA.[1−5] The behavior of the gradient term responsible for the greater stability of methane and ethane fragments, relative to *n*-alkanes, is also related to known trends of GGAs for the repulsive walls of van der Waals potential energy curves.[27−30] This also agrees with previous results for agostic interactions, characterized by slowly varying density, where the LDA was found to perform well.[31]

As a more dramatic example of the sensitivity of DFT results to large reduced-gradient changes, we show that the gradient term is also responsible for the errors in Diels−Alder barrier heights seen with GGA-based hybrid functionals, such as PBE0.[32] For example, consider the four possible Diels−Alder reactions between ethylene or acetylene and 1,3-cyclohexadiene or cyclopentadiene.[33] These barrier heights demonstrate the gradient dependence more clearly than the reaction-enthalpy errors investigated in our previous study,[34] because the incipient C−C bonds are only partially formed at the transition state, so there remain two clearly separated but interacting fragments. Unlike the isodesmic reactions, the bonding is not conserved between the reactants and transition state, so hybrid functionals are needed to avoid the systematic overbinding of the LDA or GGA functionals. In general, for hybrid functionals of the PBE0-type (using 25% exact exchange, 75% GGA exchange, and PBE correlation), the DFT barriers follow the pattern B88 > PBE > PBEsol (see Table 2). The PBEsol hybrid gives barriers in closest agreement with reference data obtained from CCSD(T)/aug-cc-pVDZ calculations, using B3LYP/6-31G(2df,p) geometries.[24,25]

These reactions are characterized by the formation of bicyclic products, and there are consequently large changes in density gradient between reactants and either the transition state or final products. As the separated reactants approach the transition state, the reduced gradient decreases substantially. Plots of *s* versus ρ are shown in Figure 3, and NCI isosurfaces for the transition states, obtained using NCIplot,[17] are shown in Figure 4. The blue isosurface regions reveal the partially formed carbon−carbon bonds.

Since GGA exchange preferentially stabilizes large-gradient regions, we expect B88, and to a lesser extent PBE, to destabilize the transition state, relative to the separated reactants, overestimating the barrier height. To assess the relationship between gradient changes and the predicted barrier heights, calculations were performed on the separated reactants at geometries matching the transition state (to account for monomer distortion). Considering only integration grid points where the reduced gradient changed by 10% or more between the reactants and transition state recovers 99% of the exchange-energy differences between the three GGAs for these barriers. As for the *n*-alkane isodesmic reactions, long-range exact exchange avoids this sensitivity to the GGA gradient term and greatly improves agreement with reference data.[34]

In conclusion, we have defined a new isodesmic reaction (eq 6), which allowed us to demonstrate that the energy differences between *n*-alkanes and ethane units come from localized interactions between contiguous CH_2 units in the *n*-alkane, i.e., from 1,3 interactions. Furthermore, taking into account that the DFT energy is determined from the ground-state electron density, we introduce a unique analysis based on the density and its gradient. GGAs give systematic errors for these noncovalent interactions due to small changes in density coupled with large changes in reduced gradient between *n*-alkane reactants and ethane products. The reduced gradient values are larger for ethane than propane (and longer *n*-

alkanes), so the exchange energy will be lower. Therefore, propane is destabilized, relative to ethane, giving a systematic energy error for each propane unit in an *n*-alkane. Integration grid points with a 5% reduced-gradient change between ethane and propane are responsible for over 80% of the observed errors in isodesmic reaction energies. For the case of Diels–Alder addition barriers, 99% of the energy difference between the B88, PBE, and PBEsol GGAs is recovered for grid points with a 10% reduced-gradient change. While the gradient term in GGAs is essential for accurate atomization energies, it can lead to systematic errors for reactions in which low-density regions experience large gradient changes between reactants and products. Range-separated functionals with short-range GGA and long-range Hartree–Fock do not include the problematic contributions from gradient terms, explaining their improved performance when combined with the dispersion corrections needed to fully account for the stabilization of noncovalent interactions.

AUTHOR INFORMATION

Corresponding Author

*E-mail: ejohnson29@ucmerced.edu.

Notes

The authors declare no competing financial interest.

ACKNOWLEDGMENTS

Support from the Office of Naval Research (N00014-09-0576) and the National Science Foundation (CHE-09-11119) (W.Y.) is greatly appreciated. J.C.-G. thanks the Spanish Ministry of Education under EDU/2253/2010 for financial support.

REFERENCES

(1) Wodrich, M. D.; Corminboeuf, C.; Schleyer, P. v. R. *Org. Lett.* **2006**, *8*, 3631–3634.
(2) Wodrich, M. D.; Wannere, C. S.; Mo, Y.; Jarowski, P. D.; Houk, K. N.; Schleyer, P. v. R. *Chem.—Eur. J.* **2007**, *13*, 7731–7744.
(3) Song, J.-W.; Tsuneda, T.; Sato, T.; Hirao, K. *Org. Lett.* **2010**, *12*, 1440–1443.
(4) Grimme, S. *Org. Lett.* **2010**, *12*, 4670–4673.
(5) Steinmann, S. N.; Wodrich, M. D.; Corminboeuf, C. *Theor. Chem. Acta.* **2010**, *127*, 429–442.
(6) Perdew, J. P.; Wang, Y. *Phys. Rev. B.* **1992**, *45*, 13244–13249.
(7) Perdew, J. P.; Burke, K.; Ernzerhof, M. *Phys. Rev. Lett.* **1996**, *77*, 3865–3868.
(8) Perdew, J. P.; Ruzsinszky, A.; Csonka, G. I.; Vydrov, O. A.; Scuseria, G. E.; Constantin, L. A.; Zhou, X.; Burke, K. *Phys. Rev. Lett.* **2008**, *100*, 136406.
(9) Becke, A. D. *Phys. Rev. A.* **1988**, *38*, 3098–3100.
(10) Grimme, S. *Angew. Chem., Int. Ed.* **2006**, *45*, 4460–4464.
(11) Grimme, S.; Steinmetz, M.; Korth, M. *J. Org. Chem.* **2007**, *72*, 2118–2126.
(12) Csonka, G. I.; Ruzsinszky, A.; Perdew, J. P.; Grimme, S. *J. Chem. Theory Comput.* **2008**, *4*, 888–891.
(13) Karton, A.; Gruzman, D.; Martin, J. M. L. *J. Phys. Chem. A.* **2009**, *113*, 8434–8447.
(14) Shamov, G. A.; Budzelaar, H. M.; Schreckenbach, G. J. *Chem. Theory Comput.* **2010**, *6*, 477–490.
(15) Brittain, D. R. B.; Lin, C. Y.; Gilbert, A. T. B.; Izgorodina, E. I.; Gill, P. M. W.; Coote, M. L. *Phys. Chem. Chem. Phys.* **2009**, *11*, 1138–1142.
(16) Johnson, E. R.; Keinan, S.; Mori-Sánchez, P.; Contreras-García, J.; Cohen, A. J.; Yang, W. *J. Am. Chem. Soc.* **2010**, *132*, 6498–6506.
(17) Contreras-García, J.; Johnson, E. R.; Keinan, S.; Chaudret, R.; Piquemal, J.-P.; Beratan, D. N.; Yang, W. *J. Chem. Theory Comput.* **2011**, *7*, 625–632.
(18) Contreras-García, J.; Johnson, E. R.; Yang, W. *J. Phys. Chem. A.* **2011**, *115*, 12983–12990.
(19) Becke, A. D. *J. Chem. Phys.* **1986**, *84*, 4524–4529.
(20) Becke, A. D.; Dickson, R. M. *J. Chem. Phys.* **1990**, *92*, 3610–3612.
(21) Curtiss, L. A.; Redfern, P. C.; Raghavachari, K.; Pople, J. A. *J. Chem. Phys.* **2001**, *114*, 108–117.
(22) Johnson, E. R.; Mackie, I. D.; DiLabio, G. A. *J. Phys. Org. Chem.* **2009**, *22*, 1127–1135.
(23) Gronert, S. *Chem.—Eur. J.* **2009**, *15*, 5372–5382.
(24) Becke, A. D. *J. Chem. Phys.* **1993**, *98*, 5648–5652.
(25) Lee, C.; Yang, W.; Parr, R. G. *Phys. Rev. B* **1988**, *37*, 785–789.
(26) Frisch, M. J.; Trucks, G. W.; Schlegel, H. B.; Scuseria, G. E.; Robb, M. A.; Cheeseman, J. R.; Scalmani, G.; Barone, V.; Mennucci, B.; Petersson, G. A.; Nakatsuji, H.; Caricato, M.; Li, X.; Hratchian, H. P.; Izmaylov, A. F.; Bloino, J.; Zheng, G.; Sonnenberg, J. L.; Hada, M.; Ehara, M.; Toyota, K.; Fukuda, R.; Hasegawa, J.; Ishida, M.; Nakajima, T.; Honda, Y.; Kitao, O.; Nakai, H.; Vreven, T.; Montgomery, J. A., Jr.; Peralta, J. E.; Ogliaro, F.; Bearpark, M.; Heyd, J. J.; Brothers, E.; Kudin, K. N.; Staroverov, V. N.; Kobayashi, R.; Normand, J.; Raghavachari, K.; Rendell, A.; Burant, J. C.; Iyengar, S. S.; Tomasi, J.; Cossi, M.; Rega, N.; Millam, J. M.; Klene, M.; Knox, J. E.; Cross, J. B.; Bakken, V.; Adamo, C.; Jaramillo, J.; Gomperts, R.; Stratmann, R. E.; Yazyev, O.; Austin, A. J.; Cammi, R.; Pomelli, C.; Ochterski, J. W.; Martin, R. L.; Morokuma, K.; Zakrzewski, V. G.; Voth, G. A.; Salvador, P.; Dannenberg, J. J.; Dapprich, S.; Daniels, A. D.; Farkas, O.Foresman, J. B.; Ortiz, J. V.; Cioslowski, J.; Fox, D. J. *Gaussian 09*, revision B.01; Gaussian, Inc.: Wallingford, CT, 2010.
(27) Pérz-Jordá, J. M.; Becke, A. D. *Chem. Phys. Lett.* **1995**, *233*, 134–137.
(28) Zhang, Y.; Pan, W.; Yang, W. *J. Chem. Phys.* **1997**, *107*, 7921–7925.
(29) Lacks, D. J.; Gordon, R. G. *Phys. Rev. A.* **1993**, *47*, 4681–4690.
(30) Kannemann, F. O.; Becke, A. D. *J. Chem. Theory Comput.* **2009**, *5*, 719–727.
(31) Tognetti, V.; Joubert, L.; Cortona, P.; Adamo, C. *J. Phys. Chem. A* **2009**, *113*, 12322–12327.
(32) Rulíšek, L.; Šebek, A.; Havlas, Z.; Hrabal, R.; Čapek, P.; Svatoš, A. *J. Org. Chem.* **2005**, *70*, 6295–6302.
(33) Pieniazek, S. N.; Clemente, F. R.; Houk, K. N. *Angew. Chem., Int. Ed.* **2008**, *47*, 7746–7749.
(34) Johnson, E. R.; Mori-Sánchez, P.; Cohen, A. J.; Yang, W. *J. Chem. Phys.* **2008**, *129*, 204112.